THE JOURNAL OF COMPARATIVE NEUROLOGY 500:322–338 (2007)

Parallel Thalamocortical Pathways for Echolocation and Passive Sound Localization in a Gleaning Bat, *Antrozous pallidus*

KHALEEL A. RAZAK, WEIMING SHEN, TERESE ZUMSTEG, AND ZOLTAN M. FUZESSERY*
Department of Zoology and Physiology, University of Wyoming, Laramie, Wyoming 82071

ABSTRACT

We present evidence for parallel auditory thalamocortical pathways that serve two different behaviors. The pallid bat listens for prey-generated noise (5–35 kHz) to localize prey, while reserving echolocation [downward frequency-modulated (FM) sweeps, 60–30 kHz] for obstacle avoidance. Its auditory cortex contains a tonotopic map representing frequencies from 6 to 70 kHz. The high-frequency (BF > 30 kHz) representation is dominated by FM sweep-selective neurons, whereas most neurons tuned to lower frequencies prefer noise. Retrograde tracer injections into these physiologically distinct cortical regions revealed that the high-frequency region receives input from the suprageniculate (SG) nucleus, but not the ventral division of the medial geniculate body (MGBv), in all experiments (n = 9). In contrast, the low-frequency region receives tonotopically organized input from the MGBv in all experiments (n = 16). Labeling in the SG was observed in only two of these experiments. Both cortical regions also receive sparse inputs from medial (MGBm) and parts of the dorsal division (MGBd) outside the SG. These results show that the low- and high-frequency regions of a single tonotopic map receive dominant inputs from different thalamic divisions. Within the low-frequency region, most neurons are binaurally inhibited, and an orderly map of interaural intensity difference (IID) sensitivity is present. We show that the input to the IID map arises from topographically organized projections from the MGBv. As observed in other species, a frequency-dependent organization is observed in the lateromedial direction in the MGBv. These data demonstrate that MGBv-to-auditory cortex connections are organized with respect to both frequency and binaural selectivity. J. Comp. Neurol. 500:322–338, 2007.

Indexing terms: segregated pathways; auditory cortex; medial geniculate body; suprageniculate; binaural sensitivity

In the auditory system, parallel thalamocortical pathways arise from three distinct divisions of the medial geniculate body (MGB; for review see Winer et al., 2005). Thalamocortical connections include a tonotopic pathway through the MGBv (ventral division), a multisensory pathway through the MGBm (medial division), and a non-tonotopic pathway through the MGBd (dorsal division, Raczkowski et al., 1976; Andersen et al., 1980; Morel and Imig, 1987; for review see Imig and Morel, 1983; Rouiller, 1997). These parallel pathways are purported to serve different functions in hearing. The pathway from the MGBv to the primary auditory cortex is tonotopically organized and forms the cortical substrate for functional subregions within isofrequency contours (for review see Brugge, 1985; Read et al., 2002). The pathway through the MGBm is implicated in multisensory integration and learning (Wepsic, 1966; Gerren and Weinberger, 1983; Edeline and Weinberger, 1992; Bordi and LeDoux, 1994;

Grant sponsor: National Institute of Deafness and Other Communication Disorders; Grant number: R01 DC05202; Grant number: INBRE P20 RR0 16474-04.

*Correspondence to: Zoltan M. Fuzessery, Department 3166, Zoology and Physiology, University of Wyoming, 1000 East University Avenue, Laramie, WY 82071. E-mail: zmf@uwyo.edu

Received 9 March 2006; Revised 9 June 2006; Accepted 17 August 2006
DOI 10.1002/cne.21178
Published online in Wiley InterScience (www.interscience.wiley.com).

for review see Hu, 2003). The pathway through the MGBd may be involved in representing complex sounds (Aitkin and Dunlop, 1968; Olsen and Suga, 1991; Schuller et al., 1991; Wenstrup and Grose, 1995; Radtke-Schuller, 2004; Radtke-Schuller et al., 2004).

Within this framework of parallel pathways, there are differences in the organization of the MGB between bats and nonchiropterans. For instance, the suprageniculate nucleus (SG), a part of the MGBd, contains multisensory neurons but, in nonchiropteran species, is dominated by visual input from the superior colliculus (Calford and Aitkin, 1983; Tanaka et al., 1985; Katoh and Benedek, 1995; Katoh et al., 1995; Benedek et al., 1997). Only in bats does the SG receive strong input from the central nucleus of the inferior colliculus (ICc; Wenstrup et al., 1994). Extralemniscal sources also send strong projections to the SG (Casseday et al., 1989; Gordon and O'Neill, 2000), suggesting that this multisensory nucleus can be usurped in auditory specialists to increase thalamic representation of both lemniscal and extralemniscal auditory inputs. Elucidation of differences in the functional organization of the MGB among bats and between bats and nonchiropterans will prove important for understanding the functional role of the MGB.

Although most bats use echolocation for obstacle avoidance and prey localization, some bats, termed *gleaners*, depend partially or completely on passive listening to localize prey. Studies of the functional organization of the MGB and thalamocortical connectivity in bats are limited to species that depend on echolocation for both prey localization and general orientation (Kobler et al., 1987; Olsen and Suga, 1991; Wenstrup et al., 1994; Wenstrup and Grose, 1995; Radtke-Schuller, 2004; Radtke-Schuller et al., 2004). Physiological studies of the organization of the auditory systems of gleaners suggest that the pathways serving passive hearing and echolocation are functionally segregated (Rubsamen et al., 1988; Fuzessery, 1994). However, the thalamic sources of cortical input that may underlie the functional segregation are unknown. The main goal of this study was to address this issue in the pallid bat (*Antrozous pallidus*), a gleaner.

The pallid bat relies on passive listening to prey-generated noise (5–35 kHz) for prey localization (Brown, 1976; Bell, 1982; Fuzessery et al., 1993), reserving its echolocation (downward frequency modulated sweeps, 60–30 kHz) for obstacle avoidance. The pallid bat's auditory system segregates the representation of the sounds used for prey localization and echolocation to the extent that we have suggested that this bat essentially has two parallel auditory systems (Fuzessery, 1994; Razak and Fuzessery, 2002). An example of the topographic representation of different response properties in the auditory cortex is shown in Figure 1 (additional examples can be found in Razak and Fuzessery, 2002). A tonotopic map representing frequencies between 6 and 71 kHz lies along the caudolateral to rostromedial axis (Fig. 1A). Most neurons with best frequencies (BF) <35 kHz respond preferentially to noise over tones (N in Fig. 1B), whereas most neurons with BF >35 kHz prefer the downward frequency-modulated (FM) sweeps (D in Fig. 1B) used in echolocation. For brevity, we will refer to these domains as the *low-frequency* and *high-frequency regions* (LFR and HFR, respectively). The first goal of this study was to identify the MGB divisions that provide input to the LFR and HFR.

In addition to its tonotopic map, the mammalian primary auditory cortex contains clusters of neurons with similar binaural properties (Imig and Adrian, 1977; Middlebrooks et al., 1980; Reale and Kettner, 1986; Kelly and Sally, 1988; Kelly and Judge, 1994; Liu and Suga, 1997; Shen et al., 1997; Recanzone et al., 1999; Rutkowski et al., 2000; Velanovsky et al., 2003; Nakamoto et al., 2004). Although the nature of thalamic input to the different cortical binaural clusters has been determined (Middlebrooks and Zook, 1983), the rules of connectivity within a single cluster have not been studied. The organization of the LFR of the pallid bat auditory cortex provides a unique opportunity to determine the nature of thalamocortical inputs to a single binaural cluster (Razak and Fuzessery, 2002). Neurons with similar binaural properties are present in clusters in the pallid bat cortex as well (e.g., Fig. 1C). A large cluster of binaurally inhibited (EI) neurons is present in the LFR. This EI cluster exhibits a systematic representation of interaural intensity difference (IID) sensitivity in which the IID at which a neuron is completely inhibited and is arranged in a roughly concentric manner (e.g., Fig. 1D,E). The second goal of this study was to determine the pattern of thalamic input to the systematic map of IID sensitivity within the EI cluster.

Abbreviations

CL	contralateral
EE	binaural excitation
EI	binaural inhibition
EO	monaural
EO/FI	mixed binaural interactions
HFR	high-frequency region of auditory cortex
IC	inferior colliculus
IL	ipselateral
LFR	low-frequency region of auditory cortex
MGBd or D	medial geniculate body, dorsal division
MGBm or M	medial geniculate body, medial division
MGBv or V	medial geniculate body, ventral division
SG	suprageniculate nucleus

MATERIALS AND METHODS

Pallid bats were collected in Arizona and New Mexico and housed in a 16 × 11 sq. ft room, where they were free to fly, and to hunt crickets or obtain mealworms from a bowl. The room was maintained on a reversed 12:12 hour light cycle. A few days prior to surgery, the bats were moved to a cage and fed mealworms to increase body weight. Only those bats (both males and females) that were flying, actively echolocating, and passively obtaining prey from the ground were used in this study. All procedures followed animal welfare guidelines required by the National Institutes of Health and the Institutional Animal Care and Use Committee.

Surgical procedures

Electrophysiological mapping of auditory cortex followed by retrograde tracer injections was successful in 22 adult pallid bats (body weight 17–24 g). The surgical procedures were identical to those reported previously (Razak and Fuzessery, 2002). Briefly, recordings were obtained from bats that were lightly anesthetized with Metofane (methoxyflurane) inhalation, followed by an intraperito-

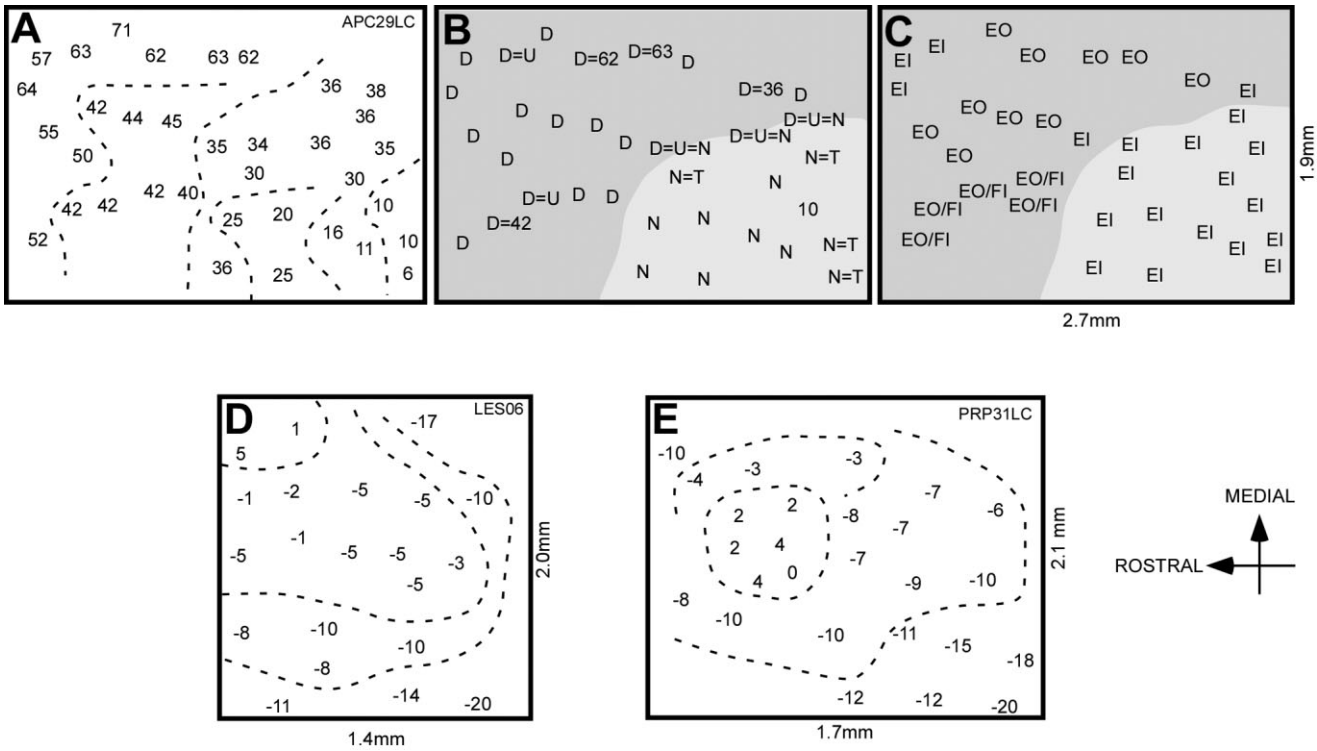

Fig. 1. Functional organization of the pallid bat auditory cortex. Maps of different response properties are shown. **A:** Best frequency map. Best frequencies between 6 and 71 kHz are represented in a caudolateral to rostromedial direction. The dashed lines delineate different BF ranges. **B:** Response selectivity map. Most neurons tuned to frequencies below 35 kHz are selective for noise (noted as N). Most neurons tuned above 35 kHz respond best to the downward FM sweep used for echolocation (noted as D). Sites noted as D = U responded equally well to both sweep directions, whereas N = T or D = T sites responded equally well to complex sounds and tones. **C:** Binaural selectivity maps. Binaural selectivity was determined by varying interaural intensity difference (IID). EI neurons showed inhibition with increasing IL intensity, whereas EO neurons showed no effect. EO/FI neurons showed facilitation and inhibition when IL intensity increased. It can be seen that neurons with different binaural properties occur in clusters. In addition, it can be seen that the LFR is dominated by EI neurons. **D,E:** Within the cluster of EI neurons in the LFR, a systematic representation of IID sensitivity is present. Neurons that are completely inhibited when the IL sound is of an intensity less than or equal to that of the CL sound (positive IIDs) are partially surrounded by neurons that require progressively louder IL sounds for complete inhibition.

neal injection of pentobarbital sodium (30 μg/g body wt) and acepromazine (2 μg/g body wt). The level of anesthesia was evaluated by the toe-pinch reflex. Surgery commenced only when this reflex was absent. In addition, this reflex was tested every 2 hours during the recording session, and an additional dose of pentobarbital sodium was injected if required. To expose the auditory cortex, the head was held in a bite bar, a midline incision was made in the scalp, and the muscles over the dorsal surface of the skull were reflected to the sides. The bat was then placed in a Plexiglas restraining device. A cylindrical aluminum-head pin was inserted through a cross bar over the bat's head and cemented in place. This pin held the bat's head secure during the recording session. The location of the auditory cortex was determined relative to the rostrocaudal extent of the midsagittal sinus, the distance laterally from the midsagittal sinus, and the location of a prominent lateral blood vessel that travels parallel to the midsagittal sinus. The size of the exposure was usually ≈2 mm^2.

Recording procedures

Experiments were conducted in a heated (85–90°F), soundproof chamber lined with anechoic foam. Bats were kept lightly anesthetized throughout the course of the experiments, with sedation maintained by inhalation of Metofane and additional pentobarbital sodium (one-third of presurgical dose) injections. Stimuli were generated by using Modular Instruments and Tucker Davis Technologies digital hardware and custom-written software (Fuzessery et al., 1991). The waveforms were amplified with a stereo amplifier and presented as closed-field stimuli through Infinity emit-K ribbon tweeters fitted with funnels that were inserted into the bat's pinnae and sealed with petroleum jelly. This procedure attenuated speaker intensity level at the opposite ear by ≥30 dB (Fuzessery, 1996). The speaker-funnel frequency response curve showed a gradual increase of 20 dB from 6 to 70 kHz, as measured with a Bruel and Kjaer 1/8 in. microphone placed at the tip of the funnel. With glass microelectrodes (1 M NaCl, 2–7 MΩ impedance), recordings were obtained at depths between 200 and 600 μm. Penetrations were made orthogonal to the surface of the cortex. Response magnitudes and poststimulus time histograms were acquired and stored with a Modular Instruments high-speed clock controlled by custom-written software. Responses were quantified as the total number of spikes elicited over 20–30 stimulus presentations.

TABLE 1. BF (Best Frequency) and Best Stimulus Indicate the Physiological Response Selectivity of the Injection Site[1]

Case	BF (kHz)	Best stimulus	Tracer	Size (μm)	MGBv			MGBd			MGBm			SG		
					25	50	75	25	50	75	25	50	75	25	50	75
1	42	FM	HRP	600	0	0	0	0	0	8	0	2	3	3	15	34
2	56	FM	HRP	520	0	0	0	0	0	0	1	0	1	0	1	8
3	38	FM	HRP	600	0	0	0	0	0	0	0	0	3	0	7	10
4	43	FM	FG	520	0	0	0	2	10	0	0	0	0	12	26	9
5	48	FM	HRP	400	0	0	0	0	2	0	1	0	0	1	8	0
6	12	N	HRP	520	21	21	14	0	0	0	2	0	0	0	0	0
7	8–10	N	HRP	600	28	44	63	3	5	4	5	5	3	4	4	3
8	16–18	N	FR	300	0	0	2	0	0	0	0	0	0	0	0	0
	25–27	N	FG	320	0	9	10	0	0	2	0	3	0	0	0	0
9	30–35	N	FG	360	0	20	12	0	0	0	0	0	0	0	0	0
	40	FM	FR	320	0	0	0	0	0	0	0	0	0	0	6	8
10	25–30	N	FG	320	0	5	17	0	2	11	0	0	2	0	0	0
	41	FM	FR	320	0	0	0	0	0	0	0	0	2	0	0	9
11	29–32	N	HRP	360	0	8	7	0	0	0	0	0	0	0	0	0
12	8–10	N	HRP	520	0	13	25	7	0	0	0	0	3	0	0	0
13	8–10	N	HRP	520	7	1	0	2	0	0	0	0	0	0	0	0
14	8–10	N	HRP	440	0	4	12	3	0	0	0	0	0	0	0	0
15	8–11	N	HRP	520	0	12	2	5	13	2	0	0	0	0	0	0
16	8–16	N	HRP	440	0	15	0	0	0	0	0	5	0	0	0	0
17	12–16	N	HRP	520	12	38	0	5	5	0	0	0	0	0	0	0
18	13–20	N	HRP	400	4	18	0	0	9	3	0	4	0	0	0	0
19	12–14	N	FG	440	0	10	58	0	3	0	0	30	28	0	0	0
20	6–8	N	HRP	520	3	12	1	2	13	16	0	6	0	2	0	2
21	42	FM	FG	400	0	0	0	2	16	16	8	15	14	28	35	47
22	40–46	FM	FG	440	0	0	0	0	12	21	0	5	16	8	42	51
23	42	FM	FG	320	0	0	0	11	16	23	3	12	3	32	47	31

[1]The number of labeled cells in the different nuclei of the MGB is shown at three locations: 25%, 50%, and 75% from the caudal edge of the MGB. FM, frequency modulated sweep; N, noise; HRP, horseradish peroxidase; FG, flurogold; FR, fluroruby.

Data acquisition

In experiments where the objective was to determine the thalamic sources of afferents to the LFR and the HFR, the functional organization of the cortex was mapped, with an emphasis on BFs and response selectivity. The BF was defined as the frequency of the tone burst (5 msec duration, including 1/1 msec rise/fall time) that elicited response at the lowest tested intensity to at least five successive presentations. Details on determining response selectivity are presented elsewhere (Razak and Fuzessery, 2002). Briefly, by using BF tone, broadband and narrowband noise, upward and downward FM sweeps as probes, the neuron was classified as selective for the stimulus that elicited at least 30% more response than the other stimuli.

In experiments in which the focus was to determine the source of thalamic inputs to the cortical IID map, IID sensitivity was mapped within the LFR by using binaurally presented broadband noise bursts. IID sensitivity curves were obtained by presenting a constant-intensity (5–10 dB above threshold) noise burst at the CL ear and increasing the intensity at the IL ear from 30 dB below to 30 dB above the CL ear intensity, in 5-dB steps (e.g., Fig. 1E–G). This procedure was repeated at one or two more CL intensities. Inhibitory threshold (IT), the IID at which the neuron was maximally suppressed, was used as a measure to quantify IID sensitivity. ITs were positive if the neuron's response was maximally suppressed when the IID favored the CL ear and negative if the neuron was maximally inhibited when the IID favored the IL ear. IT values are relatively stable across CL ear intensities (Razak and Fuzessery, 2002). Therefore, the mean IT at each recording site, obtained by averaging the ITs obtained at different CL intensities, was used to quantify IID sensitivity.

Injection of tracers

In total, 26 tracer injections were made in 23 auditory cortices. Table 1 shows the different tracers used in each experiment of this study, and the regions into which they were injected. In three of 23 cortices (cases 8–10), dual tracer injections were made. The remaining were single-injection experiments. For pressure injections, a Hamilton syringe was used to place 200 nl of horseradish peroxidase (HRP) into a glass micropipette (approximately 20 μm tip diameter). The micropipette was advanced into the electrophysiologically categorized cortical site. The micropipette was attached by an airtight connection to a 5 cc syringe with a 20 gauge needle. HRP was injected at depths of 200–600 μm. For iontophoretic injections, the tip of a glass micropipette (10–20 μm tip diameter) was filled with HRP, flurogold (FG), or fluroruby (FR) through capillary action. The micropipette was back-filled with NaCl (1 M) to permit recording and injecting with the same electrode. A Stoelting Precision Current Source or a Dagan Current Pump was used to inject HRP, FG, or FR iontophoretically (+1 to +5 μA current, 7 seconds on, 7 seconds off, 5–30 minutes) at cortical depths of 200–600 μm. The size of the injection site was determined by counting the number of 40 μm sections in the rostrocaudal direction that showed a continuous band of the tracer. The injection sites were typically between 300 and 600 μm in diameter (Table 1). The IT of the injection site was taken as the average of the ITs within 700 μm of the center of the injection to take into account the spread of the tracer and possible shrinkage of tissue resulting from fixation.

Identification of retrogradely labeled neurons in the thalamus

After a survival period of 4–6 days, the bat was lethally anesthetized with pentobarbital sodium and perfused intracardially with phosphate-buffered saline (PBS, pH 7.4; 30–50 ml, ice-cold). The brain was fixed with 0.1 M phosphate-buffered 1% paraformaldehyde, 1.25% glutaraldehyde solutions (80–100 ml, ice-cold) for the HRP experiments and with 0.1 M phosphate-buffered 4% paraformaldehyde (80–100 ml, ice-cold) for the FG and dual-

tracer-injection experiments. The perfusion rate was between 3 and 4 ml/minute. The brain was removed after measurements of the cortical exposure were made and refrigerated overnight in 30% sucrose (in 0.1 M phosphate buffer). Forty μm thick frozen coronal sections were collected in 0.1 M phosphate buffer. In the HRP experiments, all sections were reacted for HRP by using the tetramethyl benzidine (TMB) protocol. After reaction, the sections were rinsed in cold acetate buffer (pH 3.3) and mounted onto slides from the buffer. Alternate sections were counterstained with neutral red or cresyl violet to identify various divisions of the MGB. For the FG/FR experiments, alternate sections were mounted onto slides from PBS. The remaining series of sections were stained with cresyl violet. After coverslipping with permount (for HRP, cresyl violet, neutral red) or DPX (for FG/FR), the slides were viewed under either bright/darkfield (HRP) or fluorescent (FG/FR) illumination. Sections were observed under a Nikon Eclipse E800 brightfield microscope. Fluorescently labeled cells were observed by switching from a UV-2E/C filter to detect FG (excitation wavelength 340–380 nm) to a Y-2E/C filter for detection of FR (excitation wavelength 540–580 nm). Images were adjusted for contrast and brightness in either Canvas X (ACD systems) or Photoshop 6.0 (Adobe).

In experiments in which the objective was to determine the thalamic input to the HFR and the LFR, the location of retrogradely labeled cells within the various divisions of the MGB was noted. In experiments in which the objective was to determine the thalamic sources to the cortical IID map, the number of retrogradely labeled cells in each section relative to the total number of cells stained across the rostrocaudal extent of the MGB was determined for each division. As there were individual differences in the size of the MGB, the rostrocaudal (R-C) position of each section was normalized to the maximum rostrocaudal extent of the MGB in each animal. The R-C position of the maximum number of retrogradely labeled cells, termed *peak R-C position*, was determined to evaluate whether there was any relationship to the mean IT of the injection site.

RESULTS

Organization of the MGB

Cell size, darkness of staining, and packing density in Nissl- or neutral red-stained sections were used to determine the boundaries of various divisions of the MGB. The three major divisions described in other species (Morest, 1964) are present in the pallid bat MGB: ventral (MGBv), dorsal (MGBd), and medial (MGBm; Fig. 2). The MGBv contains a high packing density of cells with similar sizes. The MGBm has a wider range of cell sizes and a lower packing density. The lower cell density in the MGBm can be seen in the Nissl-stained section shown in Figure 2C. The boundary between MGBv and MGBm based on these criteria fits closely with a more detailed analysis of the pallid bat MGB with Nissl, protargol, and hematoxylin stains (Shen, 1996). The protargol-stained section shown in Figure 2B reveals that the MGBv is mostly devoid of fibers, whereas the other three divisions contain fiber stain, the most prominent being the SG nucleus. The SG is prominent; its large darkly stained cells have a distinctive appearance in Nissl sections. It is located dorsal to the MGBm, and medially in the MGBd. Although it was relatively easy to distinguish the SG from rest of the MGBd and MGBv, the boundary between MGBd and MGBv was less obvious based on Nissl or neutral red stains. However, luxol fast blue, neutral red stained sections show that MGBv stains weakly for myelin, whereas the MGBd contains fibers that run in a dorsomedial to ventrolateral direction. The boundary between the dorsal and the ventral divisions was drawn based on myelin staining (Shen, 1996).

Thalamic sources of inputs to cortical HFR and LFR

The HFR receives a prominent input from the SG, but none from the MGBv. In all experiments that targeted the HFR, retrogradely labeled cells were found in the SG (Table 1). Figure 3 shows retrograde labeling in two experiments (case 21 and 22) in which FG was injected in the HFR. The injection sites in both experiments had BF about 42–45 kHz and were selective for downward FM sweeps. In both experiments, labeling was observed predominantly in the SG. Labeling was also observed in the MGBd and MGBm, but not in the MGBv. Figure 4 shows labeling in four experiments in which either HRP or FG was injected into the HFR. In all four experiments, retrogradely labeled neurons were found predominantly in the SG, but not the MGBv. Labeled neurons were also found in the MGBd (in 6/10 experiments) and the MGBm (in 8/10 experiments; Table 1). No trends were observed in terms of the BFs of the injection site and locations of retrogradely labeled cells. Injections made in the HFR with BFs about 38, 40, and 56 kHz resulted in labeled cells at similar MGB locations within the SG. These results show that the HFR neurons receive inputs primarily from the SG, sparsely from the MGBd and MGBm, and not from the MGBv.

Injections in the LFR labeled neurons primarily in MGBv, sparsely in MGBd and MGBm, but rarely in the SG (Table 1). Figure 5 shows three experiments in which tracers were injected into the LFR. In the first two experiments (cases 6, 7), a single HRP injection was made in the LFR in which BFs were between 8 and 12 kHz. In the third experiment (case 8), FG and FR were injected in the LFR at different frequency representations. FR was injected in LFR with BFs of 16–18 kHz, and FG was injected in LFR with higher BFs of 25–30 kHz. In all three experiments, labeled cells were observed mainly in the MGBv, with sparse MGBm and MGBd labeling. The SG was not labeled in these experiments. Labeling of SG neurons was observed in only two of 16 experiments (cases 7 and 20) in which injections were made in the LFR. In the FG/FR experiment (case 8), the 16–18-kHz injection labeled more laterally located MGBv neurons than the 25–30-kHz injection, suggesting a frequency-based MGBv-noise region connectivity in which LFR sites with low BF receive input from the lateral MGBv loci and LFR sites with high BF receive input from medial MGBv loci.

The segregation of thalamic sources of input to the HFR and the LFR in the same animal can be seen in dual-tracer experiments in which the HFR and LFR received different tracers. In two experiments, FG was injected in the LFR, and FR was injected in the HFR (Fig. 6). In both experiments, the BF within the LFR was about 30 kHz, whereas the FM region injections targeted sites with BFs about 40 kHz. Figure 6 shows that MGB neurons labeled with FG

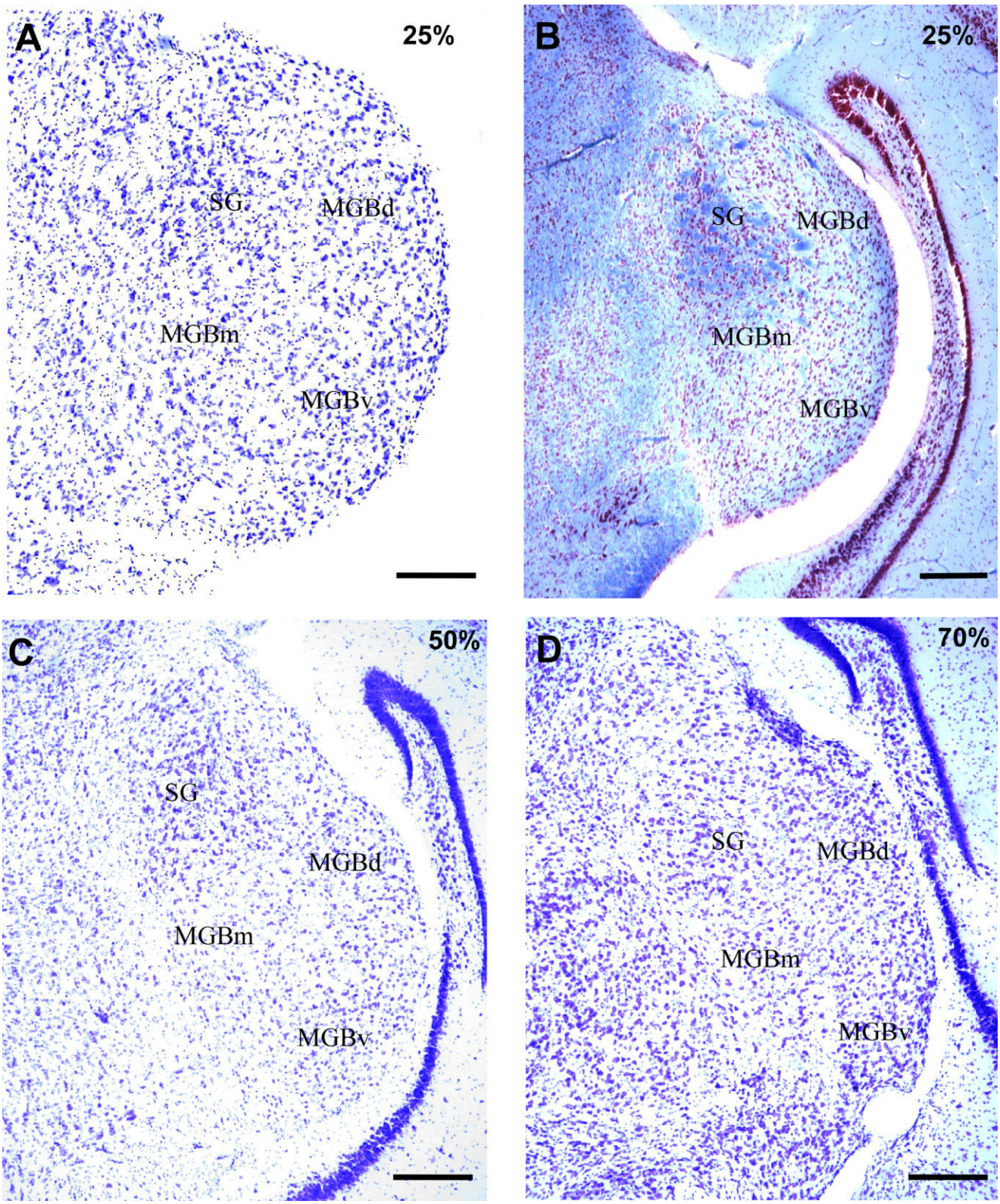

Fig. 2. Subdivisions of the pallid bat MGB based on the scheme of Morest (1964). **A,C,D:** Nissl-stained sections were used to demarcate various divisions of the MGB. The numbers in each section represent the percentage caudorostral location of the section within MGB. Increasing numbers denote more rostral sections in this and all subsequent figures. **B:** The protargol-stained section shows that the MGBv, but not the other three areas of the MGB, was devoid of fiber staining. Scale bars = 200 μm. [Color figure can be viewed in the online issue, which is available at www.interscience.wiley.com.]

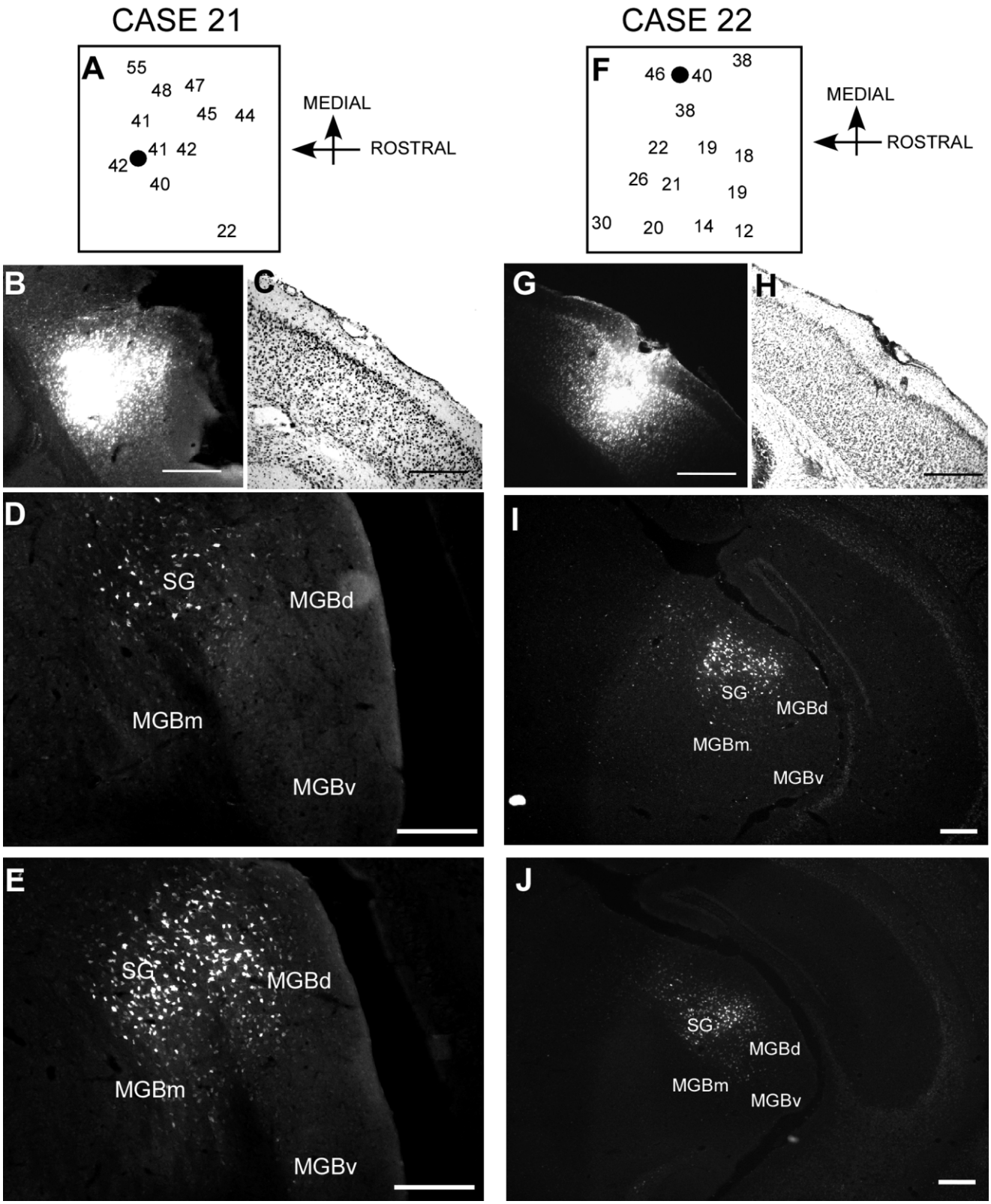

Fig. 3. Retrograde labeling in the MGB following FG injections in the HFR. **A,F:** Schematic lateral views of the BF map around the cortical injection site (solid circle). **B,G:** Coronal sections of the cortical injection site. **C,H:** Coronal Nissl-stained sections 40 μm rostral to the injection sites. Case 21: The injection site had BF = 41–42 kHz and was selective for downward FM sweeps. Sections at 25% (**D**) and 70% (**E**) caudorostral extent of the MGB show labeled neurons mostly in the SG. The MGBd and MGBm were also labeled. Case 22: The injection site had BF = 40–46 kHz and was selective for downward FM sweeps. Sections at 40% (**I**) and 60% (**J**) MGB show labeled neurons in the SG and MGBd. No labeled cells were seen in the MGBv in both experiments. Scale bars = 200 μm in B,C,G,H; 400 μm in D,E,I,J.

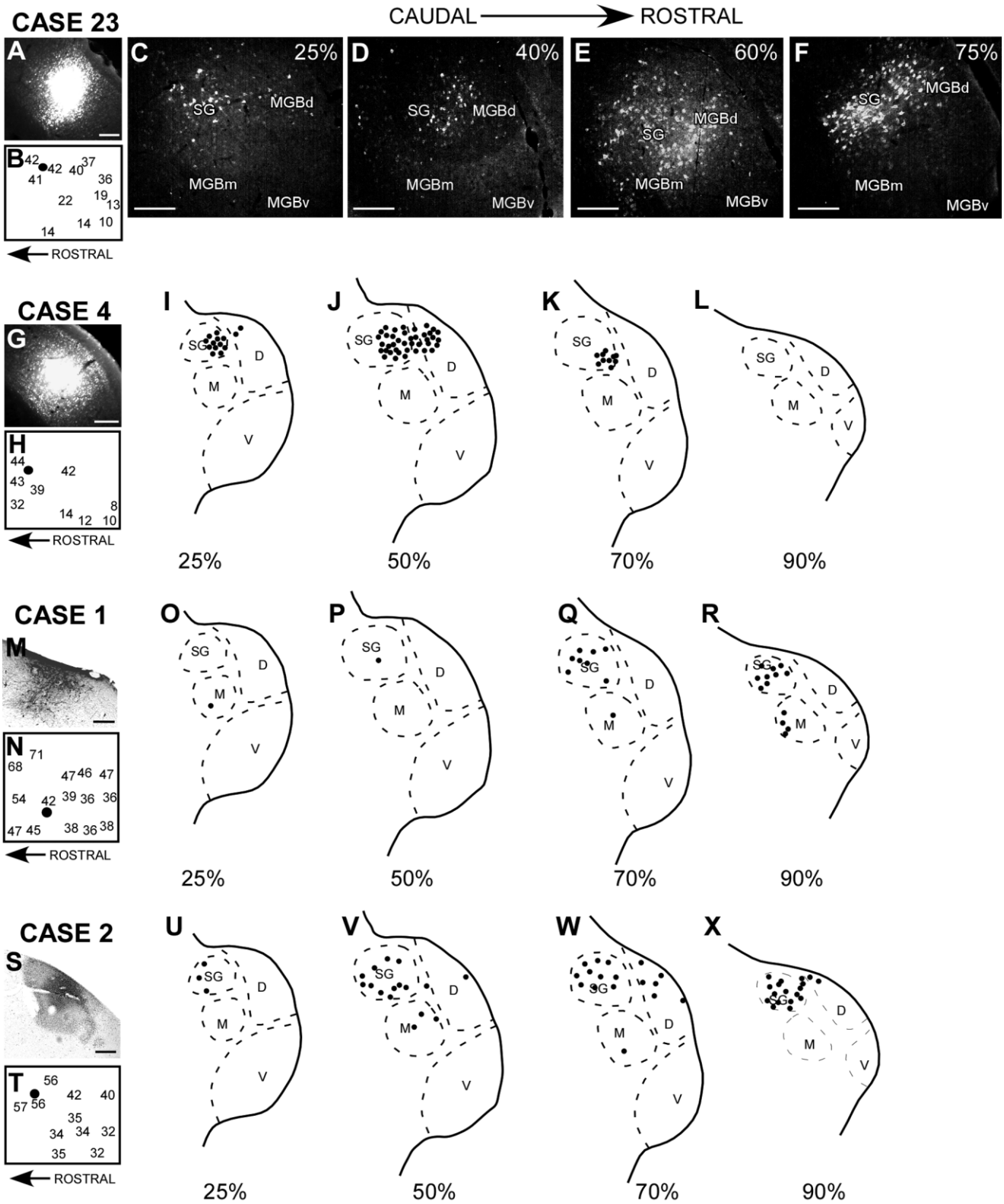

Fig. 4. HFR receives input from the suprageniculate nucleus, but not the MGBv. **A,G,M,S:** Coronal sections showing cortical injections in the HFR. **B,H,N,T:** Schematic lateral views of the BF map around the injection site. **C–F:** Photomicrographs of coronal sections at four different rostrocaudal levels of the MGB. **I–L,O–R,U–X:** Schematics of coronal sections through the MGB. In this and subsequent figures, each dark circle represents one or two labeled neuron(s). Case 23: FG injection in the 41–42-kHz HFR. Case 4: FG injection in the 43-kHz HFR. Case 1: HRP injection in the 42-kHz HFR. O–R: Case 2: HRP injection in 56-kHz HFR. Labeled neurons were present mostly in the SG. MGBd and MGBm also had a few retrogradely labeled cells. No labeling was observed in the MGBv in all four experiments. Scale bars = 200 μm in A,G,M,S; 100 μm in C–F.

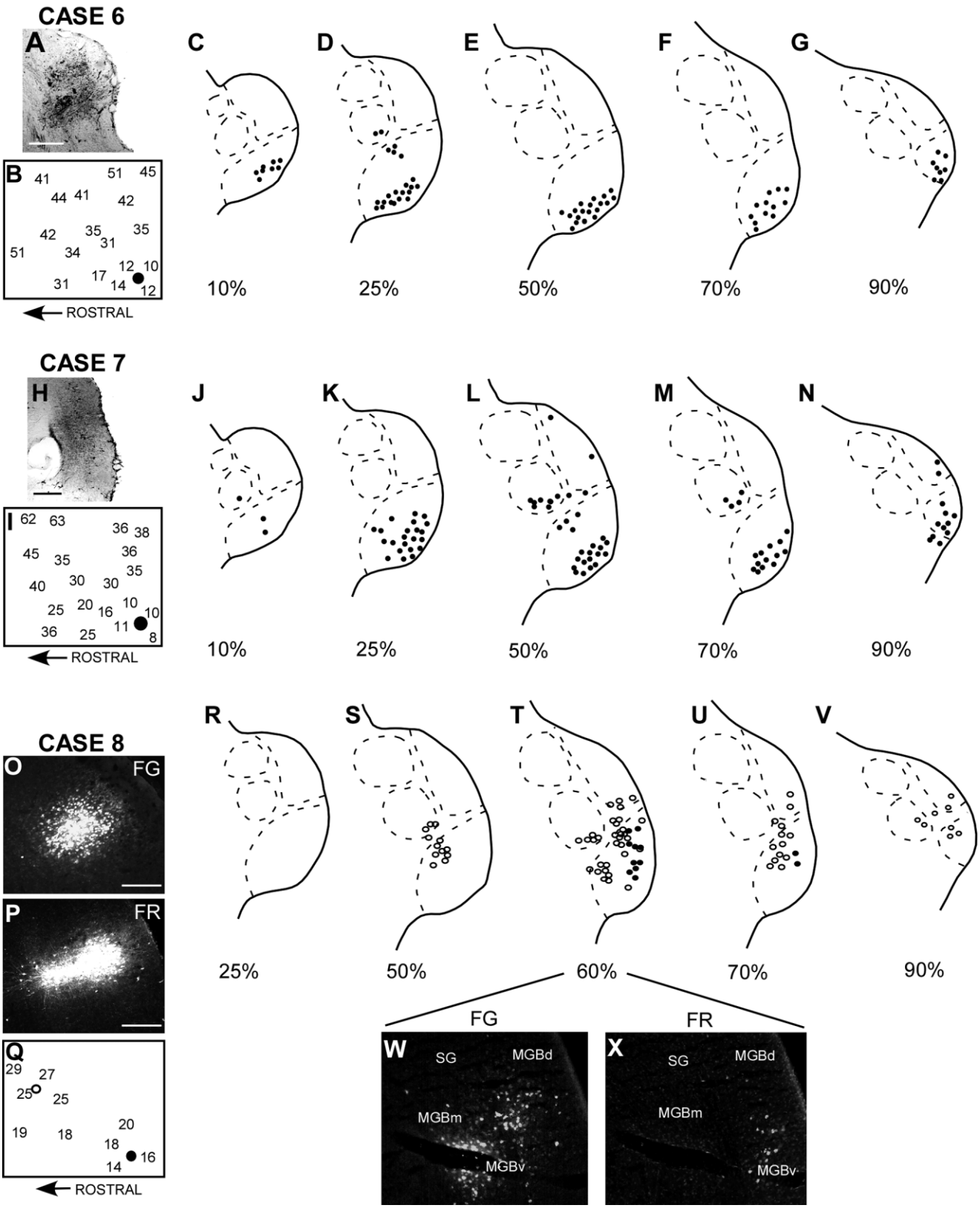

Fig. 5. LFR receives input from the MGBv, but not the suprageniculate. **A,H,O,P:** Coronal sections of cortical injections sites. **B,I,Q:** Schematic lateral views of the BF map around the injection site. Solid circles in B and I represent HRP injection sites. In Q, the solid circle represents FR injection site, and the open circle represents FG injection site. Case 6: HRP injection in the 12-kHz LFR. **C–G:** Labeling was observed mostly in the MGBv, with sparse labeling in the MGBm. Case 7: HRP injection in the 8–10-kHz LFR. **J–N:** Labeling was observed mostly in the MGBv, with sparse labeling in the MGBm and regions of MGBd outside the SG. Case 8: FG in the 25-kHz LFR and FR in the 16–18-kHz LFR. **R–V:** FG labeling was observed in medial parts of the MGBv, whereas FR was observed in more lateral parts of the MGBv. **W,X:** Photomicrographs of FG and FR label in the MGB. No labeling was seen in the SG in all three experiments. Scale bars = 400 μm in A,H; 200 μm in O,P.

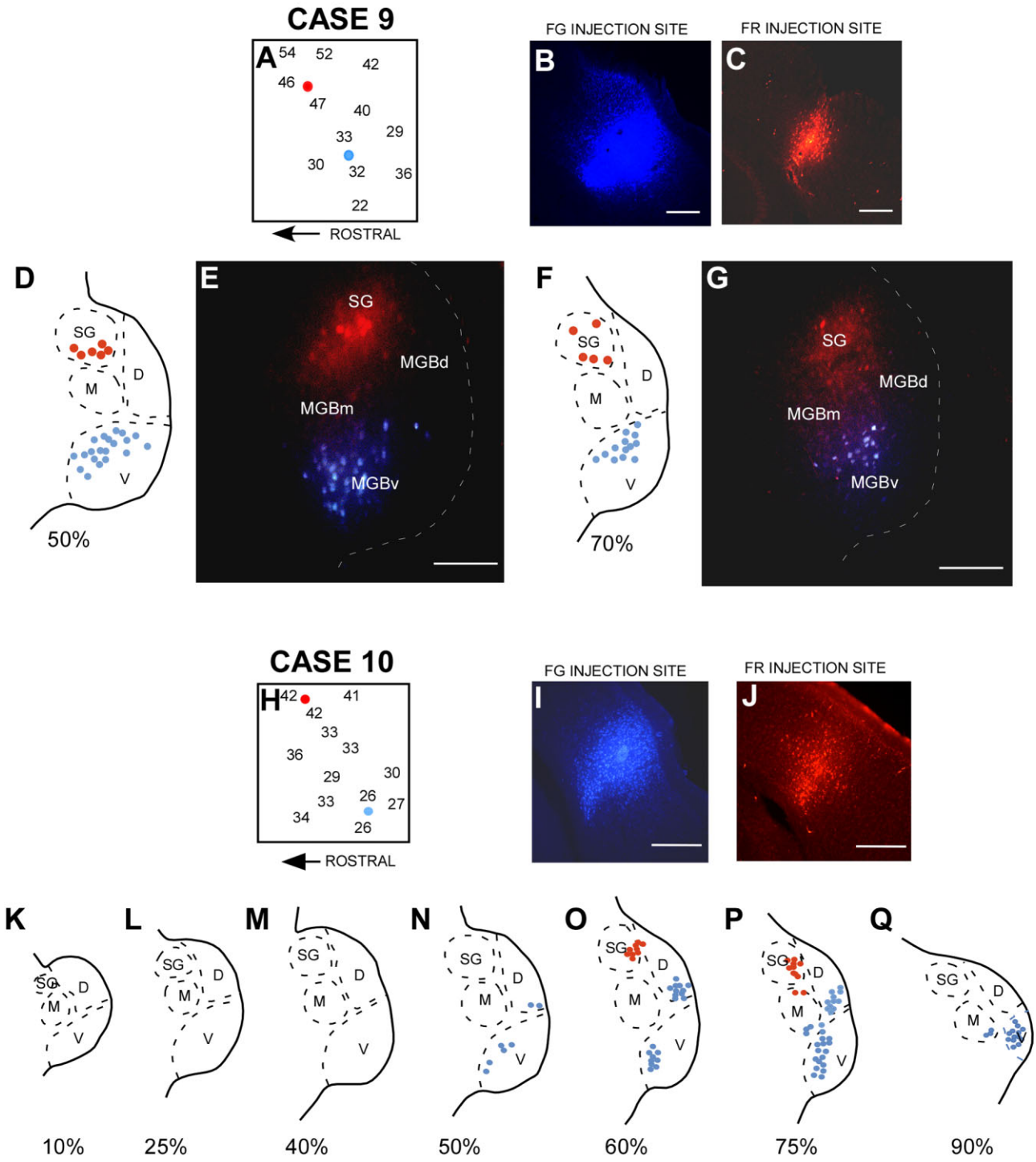

Fig. 6. Parallel thalamocortical inputs to the LFR and HFR. **A,H:** Schematic lateral view of the BF map around the cortical injection site. **B,C,I,J:** Coronal sections of the cortical injection site. Case 9: FG injection in the 30–35-kHz LFR and FR injection in the 40-kHz HFR. **D,F:** Schematic coronal views of the rostrocaudal extent of the MGB. FR (red) labeling was observed in the SG, whereas FG (blue) labeling was observed in the medial part of the MGBd. **E,G:** Photomicrographs of the sections shown in D,F. Case 10: FG in the 20–25-kHz LFR and FR in the 41-kHz HFR. **K–Q:** FR labeling (red) was seen in the SG, whereas FG labeling (blue) was seen mostly in the MGBv, with sparse labeling in the MGBd and MGBm. There was no overlap of labeling in the MGBv or the SG in both these experiments. Scale bars = 200 μm in B,C,E,G; 400 μm in I,J.

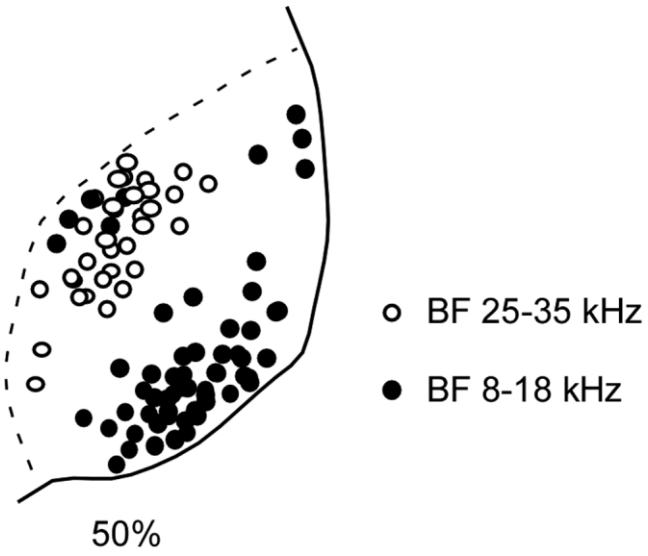

Fig. 7. Mediolateral locations of labeled MGBv neurons depend on the BF of the LFR injection site. Data were summarized from nine different experiments. When injections were made in the low-BF LFR, labeled neurons were found mostly in the lateral MGBv, whereas injections that targeted the high-BF LFR sites labeled neurons in the medial MGBv.

TABLE 2. Summary of All Experiments Used for Mapping Thalamic Input to the Cortical IID Map[1]

Experiment	BF range (kHz)	Mean BF (kHz)	IT range (dB)	Mean IT (dB)
Case 11	29–32	30	–1 to 4	2
Case 12	8–10	10	–4 to 3	0
Case 13	8–10	8	–12 to –18	–15
Case 14	13–16	14	–3 to 5	2
Case 15	10–11	10	–3 to –15	–9
Case 16	8–16	12	–3 to –12	–7
Case 17	12–16	13	–6 to –11	–8.5
Case 18	13–20	16	–10 to –15	–13
Case 19	12–14	13	4 to 9	6

[1]Physiological properties shown were recorded within 600 μm of the injection sites in the noise selective region of cortex. BF, best frequency; IT, inhibitory threshold.

TABLE 3. Percentage of Labeled Neurons in Different Caudorostral Loci of the MGBv Following Injections in the IID Map of the Cortex[1]

Case	IT (dB)	10%	20%	30%	40%	50%	60%	70%	80%
19	6	0	0	0	0	4	15	**24**	18
11	2	0	4	0	4	**16**	10	14	12
14	0	4	5	0	3	5	**21**	16	0
12	0	0	0	5	12	**13**	7	0	0
16	–7	0	0	4	**27**	22	7	0	0
17	–8.5	0	2	8	19	**26**	15	0	0
15	–9	0	0	7	12	**15**	13	4	0
18	–13	0	5	6	**26**	18	15	0	0
13	–15	5	**26**	15	5	3	0	0	0

[1]10% Is close to the caudal edge; 80% is close to the rostral edge. The cases are arranged according to the IID sensitivity of the injection site. The peak value in each case is shown in boldface.

were largely restricted to the MGBv and that neurons with FR were present in the SG, indicating that input to the HFR arises from the SG, whereas input to the LFR arises from the MGBv. Thus, even though the BFs of the injection sites were within 10 kHz of each other, inputs to the LFR (containing noise-selective neurons) and the HFR (containing FM sweep-selective neurons) arise from different MGB divisions. These results suggest that the cortical tonotopic map is constructed from parallel inputs from both the SG and the MGBv, with the former providing input to the high-frequency, FM sweep-selective region (>35 kHz), and the latter providing input to the low-frequency, noise-selective region (8–35 kHz).

In both experiments shown in Figure 6, the MGBv was devoid of labeling in its lateral extent. This shows that the high-BF noise-selective neurons in the LFR receive input from medial parts of the MGBv. As additional evidence of the tonotopic organization of the MGBv-LFR connections, retrogradely labeled neurons at the 50% rostrocaudal location in the MGBv from nine different experiments are shown in Figure 7. Injections made in the LFR with low BF (8–18 kHz) labeled neurons mostly in the lateral MGBv, whereas injections in the LFR with high BF (25–35 kHz) labeled neurons in the medial MGBv. Some overlap was, however, observed in two experiments (cases 6, 7, Fig. 5D,L). This may be related to the fact that frequency representation in the pallid bat cortex shows abrupt transitions from <15 kHz to >30 kHz, with an underrepresentation of 20–30 kHz (Razak and Fuzessery, 2002). It is, therefore, possible that the tracer injected in low-BF sites spread to locations with higher BF. An alternate explanation is that multiple representations of the same frequency range may be present within the MGBv. However, the frequency-based separation of labeled cells was observed in the majority of experiments. These results support the idea that a lateromedial tonotopy exists in the MGBv, with low frequencies represented laterally and high frequencies represented medially.

Sources of input to the cortical IID map

The MGBv-LFR connectivity was studied further to analyze the nature of thalamic inputs to the cortical IID map. Table 2 shows the range of physiological properties recorded at the cortical injection site for each of the nine cases used to determine the thalamic inputs to IID cortical maps. Table 3 summarizes the percentage of labeled cells in different rostrocaudal locations of the MGBv. Table 3 is organized with respect to the IT values. In all cases except for one (case 11), the mean BF of the injection site was between 8 and 16 kHz. The IT values covered the range observed in the LFR (IIDs between +8 and –18 dB; Razak and Fuzessery, 2002).

The rostrocaudal locations of retrogradely labeled cells within the MGBv varied systematically with the average IT of the cortical injection site (Fig. 8, Table 3). As the average IT of the injection sites changed from positive to more negative values, the locations of retrogradely labeled cells shifted from rostral to caudal locations (boldface in Table 3). In the three experiments shown in Figure 8 (cases 14, 16, 13), the injections targeted parts of the LFR with similar BFs but different ITs. In case 14, an HRP injection was made at a site with an average IT of +2 dB. In the MGBv, labeled cells were found between 50% and 70% of the R-C extent, with the greatest number at 60%. A few cells in the caudal MGBd were also labeled. Labeled cells formed a single cluster in the MGBv. In case 16, HRP injection was made in an area with an average IT of –7 dB. Peak labeling in the MGBv was observed in the section at 40% R-C location. In case 13, the injection site had an IT of –15 dB. The maximal number of labeled cells was found in the section at 20% in the MGBv.

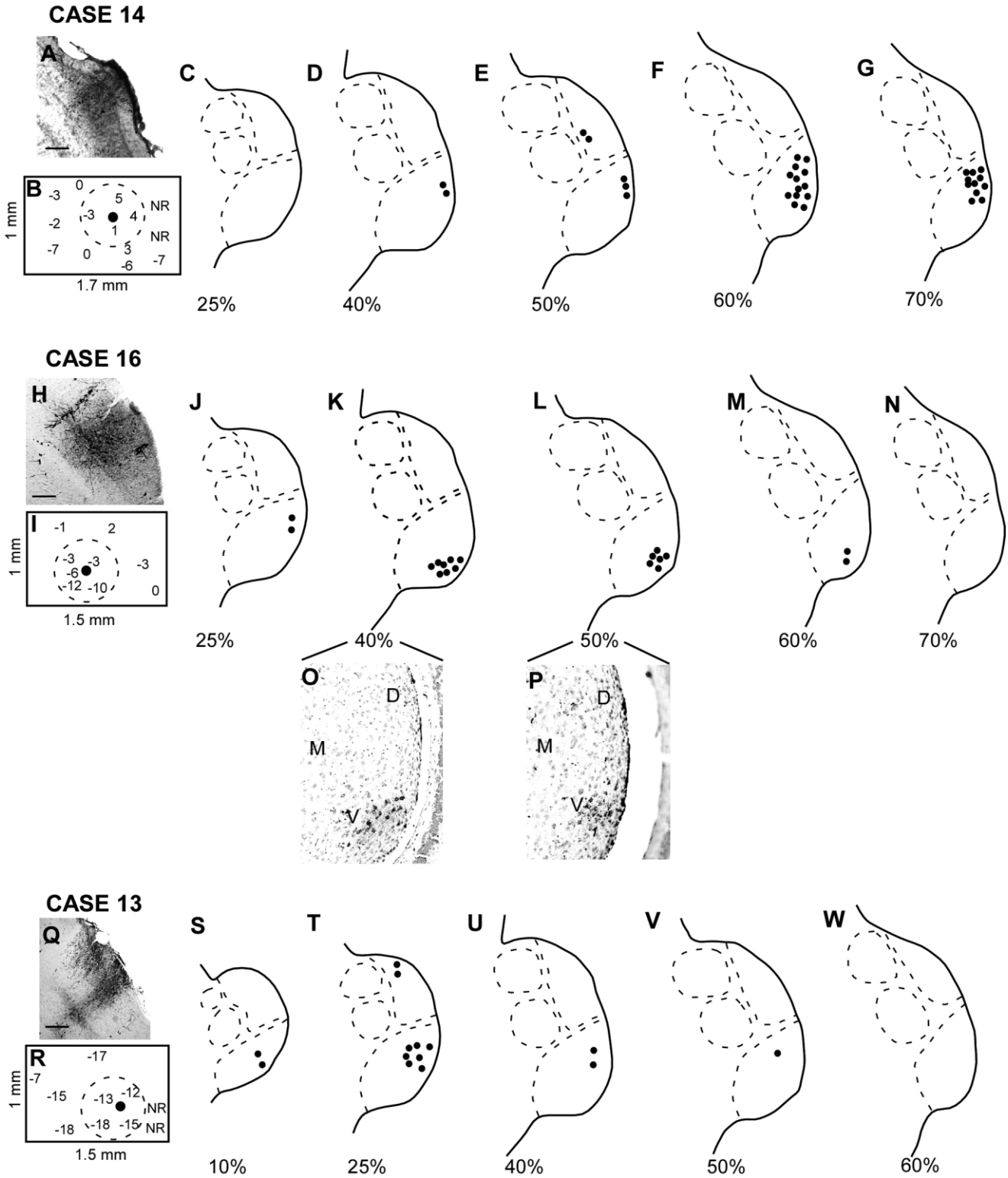

Fig. 8. Systematic thalamocortical projections to the cortical IID map within the noise region. Three experiments in which tracers were injected in cortical sites with different IID sensitivity are shown. **A,H,Q:** Coronal sections of the cortical injection site for each experiment. **B,I,R:** Schematic lateral views of the map of IID sensitivity around the injection site. The solid circle denotes the location of the injection. The IT value is the average of ITs present within 700 μm of the injection site (dashed circle). NR, no response (indicative of the caudal edge of the auditory cortex determined with our stimulus set). Case 14: HRP injection in LFR with an average IT of +2 dB. **C–G:** Locations of labeled neurons in the MGB. Peak labeling was observed at 60–70% of the rostrocaudal extent of the MGBv. Case 16: HRP injection in LFR with an average IT of –7 dB. **J–N:** Peak labeling was observed at 40% MGB. **O,P:** Photomicrographs of sections at 40% and 50% of the rostrocaudal extent processed for HRP-TMB and counterstained with neutral red. Case 13: HRP in LFR with an average IT of –15 dB. **S–W:** Peak labeling was observed at 25% of the rostrocaudal extent of the MGBv. Comparison of these three cases shows that the locations of labeled neurons shifted systematically to more caudal locations as the IT of the injection site became more negative. Scale bars = 200 μm.

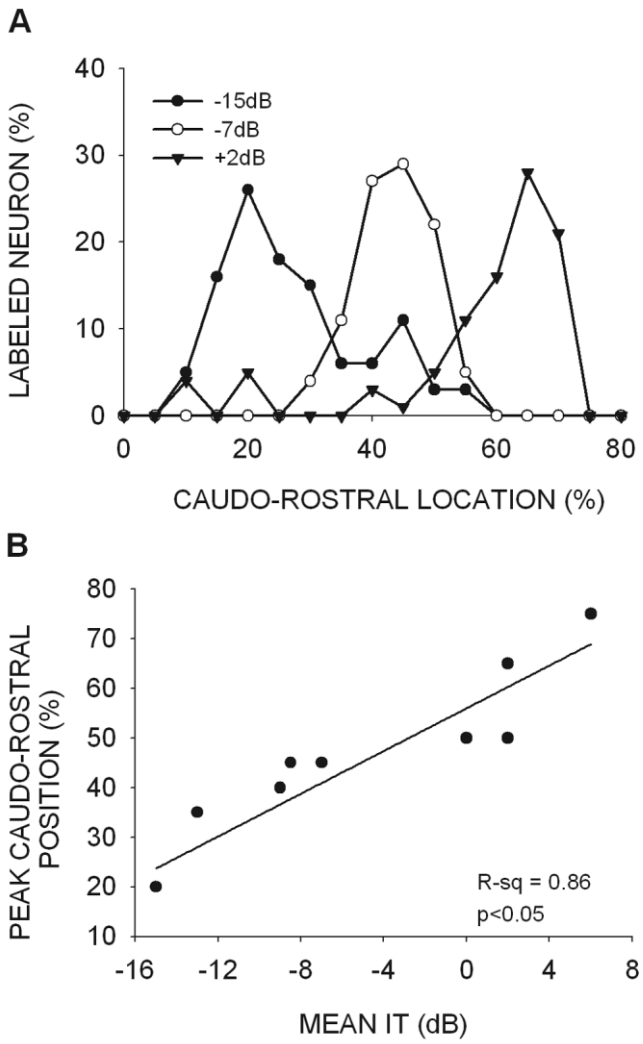

Fig. 9. Systematic thalamocortical projections to the IID map in the noise region. **A:** The rostrocaudal distribution of retrogradely labeled neurons in the MGBv from the three cases shown in Figure 8. Although overlap was seen in the rostrocaudal extent of labeled neurons, the peaks were separated. **B:** The peak rostrocaudal location of retrogradely labeled neurons was significantly correlated with the mean IT of the cortical injection site.

Figure 9A shows the percentage of labeled cells across the R-C extent of the MGBv in the three experiments shown above. Considerable overlap in the R-C extent of labeled cells can be observed in the three experiments shown in Figures 8 and 9A. This might arise either because of the overlap in the range of IT values that the injections covered (Table 1) or because the IT representation in the MGBv itself overlaps. Nevertheless, the relationship between the IID sensitivity of injection site and the R-C location of maximal number of labeled neurons, along with the presence of a single, continuous cluster of labeled neurons, supports the interpretation that a systematic representation of IID sensitivity is present in the MGBv. Figure 9B summarizes this relationship for all (n = 9) the experiments of this study. The peak rostrocaudal location, the MGBv locus with the maximal number of labeled neurons, shifts systematically with the IT of the injection site ($R^2 = 0.86$, $P < 0.05$). These results suggest that the thalamocortical connections between the MGBv and the LFR are organized with respect to IID sensitivity.

DISCUSSION

This study examined thalamocortical connections in the auditory pathway of a gleaning bat that depends on echolocation for obstacle avoidance and passive hearing for prey localization. A surprising result is that only part of the most orderly tonotopic map in the pallid bat auditory cortex receives projections from the MGBv. The HFR of the cortical tonotopic map (with FM sweep-selective neurons) and the LFR of the tonotopic map (with noise-selective neurons) receive predominant inputs from different parts of the MGB. Whereas some overlap exists in projections from the MGBm and non-SG parts of the MGBd, injections in the HFR labeled neurons mainly in the SG. The MGBv was not labeled in any experiment that targeted the HFR. Injections in the LFR labeled neurons mainly in the MGBv, but rarely in the SG. Taken together with previous physiological studies (Fuzessery, 1994; Razak and Fuzessery, 2002), these results suggest the existence of parallel colliculus-thalamus-cortex pathways that serve two different functions, namely, prey localization and echolocation. Echolocation is represented in the ventral part of the ICc, the SG in the MGB, and the HFR of the cortex. Noise used in prey localization is represented in the lateral part of the ICc, the MGBv, and the LFR of the cortex. The second major result of this study is that the connections from the MGBv to the LFR are organized systematically with respect to both frequency and IID sensitivity.

Comparison of thalamocortical connections across species

Thalamocortical connections, particularly those involving the SG, differ in animals that use passive hearing, or echolocation, or both, while hunting. In all mammals studied, the connections from the MGBv to primary auditory cortex are organized topographically (cat: Andersen et al., 1980; gerbil: Budinger et al., 2000; guinea pig: Redies et al., 1989; monkey: Luethke et al., 1989; rat: Winer et al., 1999; for review see Winer et al., 2005). The MGBd forms part of the nontonotopic pathway to the cortex, but the functional role of this connection remains unclear. In nonchiropterans, the SG, a part of the MGBd, is dominated by visual input from the SC (cat: Calford and Aitkin, 1983; Katoh and Benedek, 1995; rat: Tanaka et al., 1985). Under 15% of the neurons respond only to auditory stimuli, whereas 65% of the SG neurons respond to visual stimuli alone (Benedek et al., 1997). The entire rostrocaudal extent of the SG receives input from the SC (Katoh and Benedek, 1995). Auditory inputs to the SG may arise from the nucleus of the central acoustic tract in the brainstem and the external nucleus of the IC (Henkel, 1983; Katoh and Benedek, 1995), both of which are considered to be a part of the extralemniscal auditory pathways. The SG projects primarily to nonprimary auditory cortical areas, although sparse connections to the primary auditory cortex are found in many species (owl monkey: Morel and Kaas, 1992; macaque monkey: Hackett et al., 1998; tamarin: Luethke et al., 1989; dog: Malinowska and Kosmal, 2003; rat: Roger and Arnault, 1989).

Two species of bats that have received considerable attention in terms of their thalamocortical system are the mustached bat (Kobler et al., 1987; Suga, 1989; Olsen and Suga, 1991; Wenstrup et al., 1994; Wenstrup and Grose, 1995; Wenstrup, 1999) and the horseshoe bat (Schuller et al., 1991; Radtke-Schuller, 2004; Radtke-Schuller et al., 2004). These bats, from different families, use a CF-FM (constant frequency-frequency modulation) echolocation call for both orientation and prey detection. They show some similarities in cortical organization. Similar to all mammals studied, their primary auditory cortices contain a frequency map of the full audible range. Dorsal to the frequency map is a region specialized to extract distance information by using the delay between the outgoing pulse and the received echo (the FM-FM region in the mustached bat and the dorsal cortex in the horseshoe bat).

In the mustached bat, the MGBv represents the full audible range of the species in a tonotopic fashion (Wenstrup et al., 1994). Specializations for echolocation exist in the MGBv, such as the overrepresentation of the dominant constant-frequency harmonic, and extremely sharp tuning for the CF of the dominant harmonic. The MGBd of the mustached bat also appears to be specialized for echolocation, as suggested by the presence of combination-sensitive neurons that represent target distance (Olsen and Suga, 1991; Wenstrup and Grose, 1995). The nature of thalamic input to different cortical fields in the mustached bat is not known. In the horseshoe bat, the MGBv to primary auditory cortex connections are similar to those observed in other mammals in that the audible range is represented in the cortex through tonotopically organized connections from the MGBv. Neurons specialized for echolocation in the dorsal cortex of the horseshoe bat receive input from the MGBd (Schuller et al., 1991; Radtke-Schuller, 2004; Radtke-Schuller et al., 2004). The anatomical and physiological data from these two species of bats suggest that the MGBv has specializations for echolocation within the framework of a systematic and complete frequency map, whereas the MGBd is specialized for representing information derived from pulse-echo pairs that represent target distance.

The specializations of the SG in nonchiropterans and bats differ in the extent to which visual and auditory inputs dominate. The SG of the mustached bat receives inputs from all frequency bands of the ICc (Wenstrup et al., 1994). Only in bats does the SG receive strong input from the ICc, suggesting that the SG can be taken over to increase thalamic representation of species-specific dominant sensory modalities (Wenstrup et al., 1994). The SG also receives direct input from the auditory brainstem (nucleus of the central acoustic tract; Casseday et al., 1989; Gordon and O'Neill, 2000). In addition to broad regions of the auditory cortex, the SG of the mustached bat projects to frontal cortex, which in turn projects to the SC, suggesting a role in acousticomotor reflexes (Kobler et al., 1987). In the horseshoe bat, the SG projects to both primary and nonprimary cortical fields (Radtke-Schuller, 2004; Radtke-Schuller et al., 2004). There is overlap in projections from the SG and the MGBv to any given cortical region, but the dorsal cortical fields (nonprimary) receive most SG inputs, whereas the temporal fields (containing primary auditory cortex) receive most MGBv inputs.

Thalamocortical connections in a gleaning bat

This is the first study to examine thalamocortical connections in a gleaning bat. The emphasis of thalamocortical connections appears to be a segregation of representation of sounds used in echolocation and prey localization. The presence of parallel thalamocortical pathways originating in different divisions of the MGB and the topographic representation of frequencies in the MGBv of the pallid bat are similar to those in other mammals (Andersen et al., 1980; Redies et al., 1989; Luethke et al., 1989; Winer et al., 1999, 2005; Budinger et al., 2000). However, much of the cortical tonotopic map (BF $>$ 40 kHz), specialized for echolocation, does not receive input from the MGBv. Nearly one-third of the audible range (40–60 kHz) is represented in the cortex through connections from the SG. This is different from the other species examined, in which most of the primary tonotopic map is derived from the MGBv. An underrepresentation of the FM sweep components of the higher harmonics of the echolocation call in the MGBv is observed in the mustached bat (Wenstrup et al., 1994; Wenstrup, 1999). Therefore, how much of the audible range is represented in the MGBv differs across species, and the pallid bat may represent an extreme case in which nearly one-third of the audible range is not represented in the MGBv. In addition, the lack of projections from the MGBv to the HFR suggests that, unlike the mustached and horseshoe bats, the pallid bat MGBv might not serve echolocation.

These results raise the issue of the definition of primary auditory cortex. Primary auditory cortex is typically defined as having a continuous frequency map of the complete species-specific audible range and receiving primary input from the MGBv (Imig and Morel, 1983). Additional criteria such as short response latencies have been applied to distinguish primary from secondary cortical areas. This study examined the most systematic and continuous map of frequencies from 6 to 70 kHz, suggesting that this is the primary auditory cortex. In addition, the onset latencies are similar in the high-frequency, FM sweep-selective neurons and the low-frequency, noise-selective neurons (Razak and Fuzessery, unpublished observations). However, only part of this map receives input from the MGBv. Alternatively, it is possible that the HFR is not part of the primary tonotopic axis of the pallid bat auditory cortex. It may be a nonprimary cortical region specialized for echolocation. The lack of connections with the MGBv makes the case for the HFR as a nonprimary area. If the HFR is considered to be nonprimary auditory cortex, then the implication is that a significant part of the audible range is not represented in the primary frequency map. If the HFR is considered to be primary auditory cortex, the implication is that a major part of the primary auditory cortex receives input from outside the MGBv. The most systematic tonotopic axis of the pallid bat auditory cortex thus has a mixture of properties that are typically used to distinguish primary auditory cortex from other areas.

Functional relevance of segregated pathways

Whether or not this extreme anatomical segregation in the pallid bat thalamocortical system fits comfortably into existing operational definitions, perhaps the more salient issue is the nature of the selective pressure that would

promote this segregation. We have suggested (Fuzessery, 1994) that a parsimonious explanation for such anatomical and functional segregation within this auditory system derives from the pallid bat's need to process two streams of auditory information simultaneously when it hunts its terrestrial prey. It uses echolocation, or active listening, to sonically interrogate its surroundings, while passively listening for prey-generated sounds. The extent to which two streams of information can be separated depends on the differences in spectrum, temporal structure, and spatial location (Bregman, 1990). The sounds used in active and passive hearing are indeed distinct; prey-generated noise and FM sweeps used in echolocation differ in spectral range (8–35 kHz vs. 30–60 kHz), temporal structure (noise vs. sweep), and location (ground vs. flight path). The neural pathways serving the two auditory functions have an unusually high percentage of neurons selective for these behaviorally relevant sounds (Fuzessery, 1994; Razak and Fuzessery, 2002), perhaps serving to enhance the separation of these auditory streams. This functional segregation is complemented by anatomical segregation at the midbrain and cortical levels. In the auditory cortex, at the boundary zone of the LFR and HFR, there are functionally bimodal neurons that receive input from both pathways (Razak et al., 1999). These neurons change entire suites of response properties when stimulated with low-frequency noise or downward FM sweeps, suggesting that the two pathways compete for neural tissue when they come into anatomical contact. In effect, the pallid bat's auditory system may treat echolocation and passive hearing as auditory submodalities, and the extreme segregation of the thalamocortical pathways serving these two functions may be one expression of this strategy.

Systematic thalamocortical connections to the IID map in the LFR

Beyond tonotopy, a common feature of primary auditory cortex is the clustered organization of binaural properties. In the pallid bat cortex, a large cluster of EI (binaurally inhibited) neurons dominates the LFR (Razak and Fuzessery, 2002). This cluster contains a systematic map of IID sensitivity that may underlie a population code of sound locations (Razak and Fuzessery, 2000). Injections that targeted different IID sensitivities suggest a rostrocaudal organization of IID sensitivity (Figs. 8, 9). More caudal MGBv neurons send input to cortical loci with progressively more negative ITs. This suggests that an orderly representation of IID sensitivity is already present in the MGBv. This form of orthogonal organization may allow each isofrequency band running rostrocaudally in the MGBv to consist of a wide range of IID sensitivities. An alternate interpretation is that BF varies in both rostrocaudal and lateromedial directions. A rostrocaudal representation of frequencies has been reported in the MGBv of the tree shrew (Oliver and Hall, 1978). It is unlikely that frequency was a factor in determining the rostrocaudal locations of labeled neurons in the pallid bat, insofar as most injections were made in regions with similar BFs (8–16 kHz). Brandner and Redies (1990) showed that, in the cat, different dorsoventral loci of cortical isofrequency contours are connected with different rostrocaudal loci of the MGBv. These connections were mostly systematic, with dorsal cortical regions projecting to rostral MGBv locations and ventral cortical regions projecting to caudal MGBv locations. Similar observations were made by Roger and Arnault (1989) in the rat. The binaural response properties at the injections sites were not examined in these studies, so it is not known whether the different cortical injections targeted neurons with different binaural properties (e.g., EE vs. EI) or IID sensitivities. Our results suggest that the rostrocaudal shift in labeling observed in these studies may be related to binaural sensitivity of the injection sites.

Thalamocortical connectivity with respect to binaural properties has been studied in the cat (Middlebrooks and Zook, 1983). In the cat cortex, at least three clusters of EI neurons are present in the primary auditory cortex (Middlebrooks and Zook, 1983; Reale and Kettner, 1986; Nakamoto et al., 2004). Middlebrooks and Zook (1983) have shown that divergent thalamocortical connections may cause a single thalamic locus to project to all three bands. Also, convergence may cause a single cortical locus to receive input from multiple thalamic loci. In the pallid bat, only a single contiguous region of the MGBv was labeled following each injection in the EI cluster. This suggests that convergence is not a dominant feature of thalamocortical connections from the MGBv to the LFR EI cluster. The difference between the two species may be explained by the fact that multiple EI clusters are present in the cat cortex, whereas only a single EI cluster is present in the LFR of the pallid bat.

CONCLUSIONS

The pallid bat auditory system contains two functionally and anatomically distinct colliculus-thalamus-cortex pathways that represent two complex sounds used in two different behaviors. This parallel pathway scheme may be a neural specialization for gleaning behavior, wherein the hunting pallid bat must process, within close temporal proximity, both prey-generated noise and echoes returning from obstacles in its flight path. One way to test this idea in the future is a comparative study of gleaners. Gleaning behavior is observed across different families of bats. A comparative approach will provide insight into whether gleaning bats from different families have converged on the parallel pathway scheme as a neural substrate for the gleaning behavior.

ACKNOWLEDGMENTS

We thank G. McLellan for programming the software required for this study, Dr. Donal Skinner for help with microscopy, and Dr. Jeff Wenstrup and two anonymous reviewers for comments on earlier versions of the manuscript.

LITERATURE CITED

Aitkin LM, Dunlop CW. 1968. Interplay of excitation and inhibition in the cat medial geniculate body. J Neurophysiol 31:44–61.

Andersen RA, Knight PL, Merzenich MM. 1980. The thalamocortical and corticothalamic connections AI, AII, and the anterior auditory field (AAF) in the cat: evidence for two largely segregated systems of connections. J Comp Neurol 194:663–701.

Bell GP. 1982. Behavioral and ecological aspects of gleaning by the desert insectivorous bat, *Antrozous pallidus* (Chiroptera: Vespertilionidae). Behav Ecol Sociobiol 10:217–223.

Benedek G, Pereny J, Kovacs G, Fischer-Szatmari L, Katoh YY. 1997. Visual, somatosensory, auditory and nociceptive modality properties in the feline suprageniculate nucleus. Neuroscience 78:179–189.

Bordi F, LeDoux JE. 1994. Response properties of single units in areas of rat auditory thalamus that project to the amygdala. II. Cells receiving convergent auditory and somatosensory inputs and cells antidromically activated by amygdala stimulation. Exp Brain Res 98:275–286.

Brandner S, Redies H. 1990. The projection from medial geniculate to field AI in cat: organization in the isofrequency dimension. J Neurosci 10: 50–61.

Bregman AS. 1990. Auditory scene analysis. Cambridge, MA: MIT Press.

Brown P. 1976. Vocal communication in the pallid bat, *Antrozous pallidus*. Z Tierpsychol 41:34–54.

Brugge JF. 1985. Patterns of organization in auditory cortex. J Acoust Soc Am 78:353–359.

Budinger E, Heil P, Scheich, H. 2000. Functional organization of auditory cortex in the Mongolian gerbil (*Meriones unguiculatus*). IV. Connections with anatomically characterized subcortical structures. Eur J Neurosci 12:2452–2474.

Calford MB, Aitkin LM. 1983. Ascending projections to the medial geniculate body of the cat: evidence for multiple, parallel auditory pathways through thalamus. J Neurosci 3:2365–2380.

Casseday JH, Kobler JB, Isbey SF, Covey E. 1989. Central acoustic tract in an echolocating bat: an extralemniscal auditory pathway to the thalamus. J Comp Neurol 287:247–259.

Edeline J-M, Weinberger NM. 1992. Associative retuning in the thalamic source of input to the amygdala and auditory cortex: receptive field plasticity in the medial division of the medial geniculate body. Behav Neurosci 106:81–105.

Fuzessery ZM. 1994. Response selectivity for multiple dimensions of frequency sweeps in the pallid bat inferior colliculus. J Neurophysiol 72:1061–1079.

Fuzessery ZM. 1996. Monaural and binaural spectral cues created by the external ears of the pallid bat. Hear Res 95:1–17.

Fuzessery ZM, Gumtow RG, Lane R. 1991. A microcomputer-controlled system for use in auditory physiology. J Neurosci Methods 36:45–52.

Fuzessery ZM, Buttenhoff P, Andrews B, Kennedy JM. 1993. Passive sound localization of prey by the pallid bat (*Antrozous p. pallidus*). J Comp Physiol A171:767–777.

Gerren RA, Weinberger NM. 1983. Longterm potentiation in the magnocellular medial geniculate nucleus of the anesthetized rat. Brain Res 265(1):138–142.

Gordon M, O'Neill WE. 2000. An extralemniscal component of the mustached bat inferior colliculus selective for direction and rate of linear frequency modulations. J Comp Neurol 426:165–181.

Hackett TA, Stepniewska I, Kaas JH. 1998. Thalamocortical connections of the parabelt auditory cortex in macaque monkeys. J Comp Neurol 400:271–286.

Henkel CK. 1983. Evidence of sub-collicular auditory projections to the medial geniculate nucleus in the cat: an autoradiographic and horseradish peroxidase study. Brain Res 259:21–30.

Hu B. 2003. Functional organization of lemniscal and nonlemniscal auditory thalamus. Exp Brain Res 153:543–549.

Imig TJ, Adrian HO. 1977. Binaural columns in the primary field (A1) of cat auditory cortex. Brain Res 138:241–257.

Imig TJ, Morel A. 1983. Organization of the thalamocortical auditory system in the cat. Annu Rev Neurosci 6:95–120.

Katoh YY, Benedek G. 1995. Organization of the colliculosuprageniculate pathway in the cat: a wheat germ agglutinin-horseradish peroxidase study. J Comp Neurol 352:381–397.

Katoh YY, Benedek G, Deura S. 1995. Bilateral projections from the superior colliculus to the suprageniculate nucleus in the cat: a WGA-HRP/double fluorescent tracing study. Brain Res 669:298–302.

Kelly JB, Judge PW. 1994. Binaural organization of primary auditory cortex in the ferret (*Mustela putorius*). J Neurophysiol 71:904–913.

Kelly JB, Sally SL. 1988. Organization of auditory cortex in the albino rat: binaural response properties. J Neurophysiol 59:1756–1769.

Kobler JB, Isbey SF, Casseday JH. 1987. Auditory pathways to the frontal cortex of the mustache bat, *Pteronotus parnellii*. Science 236:824–826.

Liu W, Suga N. 1997. Binaural and commissural organization of the primary auditory cortex of the mustached bat. J Comp Physiol A181: 599–605.

Luethke LE, Krubitzer LA, Kaas JH. 1989. Connections of primary auditory cortex in the New World monkey, *Saguinus*. J Comp Neurol 285:487–513.

Malinowska M, Kosmal A. 2003. Connections of the posterior thalamic region with the auditory ectosylvian cortex in the dog. J Comp Neurol 467:185–206.

Middlebrooks JC, Zook JM. 1983. Intrinsic organization of the cat's medial geniculate body identified by projections to binaural response-specific bands in the primary auditory cortex. J Neurosci 3:203–224.

Middlebrooks JC, Dykes RW, Merzenich MM. 1980. Binaural response-specific bands in primary auditory cortex (AI) of the cat: topographical organization orthogonal to isofrequency contours. Brain Res 181:31–48.

Morel A, Imig TJ. 1987. Thalamic projections to fields A, A1, P and VP in cat auditory cortex. J Comp Neurol 265:119–144.

Morel A, Kaas JH. 1992. Subdivisions and connections of auditory cortex in owl monkeys. J Comp Neurol 318:27–63.

Morest DK. 1964. The neuronal architecture of the medial geniculate body of the cat. J Anat 98:611–630.

Nakamoto KT, Zhang J, Kitzes LM. 2004. Response patterns along an isofrequency contour in cat primary auditory cortex (AI) to stimuli varying in average and interaural levels. J Neurophysiol 91:118–135.

Oliver DL, Hall WC. 1978. The medial geniculate body of the tree shrew, *Tupaia glis*: II. connections with the neocortex. J Comp Neurol 182: 459–493.

Olsen JF, Suga N. 1991. Combination-sensitive neurons in the medial geniculate body of the mustached bat: encoding of target range information. J Neurophysiol 65:1275–1296.

Raczkowski D, Diamond IT, Winer J. 1976. Organization of thalamocortical auditory system in the cat studied with horseradish peroxidase. Brain Res 101:345–354.

Radtke-Schuller S. 2004. Cytoarchitecture of the medial geniculate body and thalamic projections to the auditory cortex in the rufous horseshoe bat (*Rhinolophys rouxi*). I. Temporal fields. Anat Embryol 209:59–76.

Radtke-Schuller S, Schuller G, O'Neill WE. 2004. Thalamic projections to the auditory cortex in the rufous horseshoe bat (*Rhinolophys rouxi*). II. Dorsal fields. Anat Embryol 209:77–91.

Razak KA, Fuzessery ZM. 2000. A systematic representation of interaural intensity differences in the auditory cortex of the pallid bat. Neuroreport 11:2919–2924.

Razak KA, Fuzessery ZM. 2002. Functional organization of the pallid bat auditory cortex: emphasis on binural organization. J Neurophysiol 87:72–86.

Razak KA, Fuzessery ZM, Lohuis TD. 1999. Single cortical neurons serve both echolocation and passive sound localization. J Neurophysiol 81: 1438–1442.

Read HL, Winer JA, Schreiner CE. 2002. Functional architecture of auditory cortex. Curr Opin Neurobiol 12:433–440.

Reale RA, Kettner RE. 1986. Topography of binaural organization in primary auditory cortex of the cat: effects of changing interaural intensity. J Neurophysiol 56:663–682.

Recanzone GH, Schreiner CE, Sutter ML, Beitel RE, Merzenich MM. 1999. Functional organization of spectral receptive fields in the primary auditory cortex of the owl monkey. J Comp Neurol 415:460–481.

Redies H, Brandner S, Creutzfeldt OD. 1989. Anatomy of the auditory thalamocortical system of the guinea pig. J Comp Neurol 282:489–511.

Roger M, Arnault P. 1989. Anatomical study of the connections of the primary auditory area in the rat. J Comp Neurol 287:339–356.

Rouiller EM. 1997. Functional organization of the auditory pathways. In Ehret G, Romand R, editors. The central auditory system. New York: Oxford University Press. p 3–96.

Rubsamen R, Neuweiler G, Sripathi K. 1988. Comparative collicular tonotopy in two bat species adapted to movement detection, *Hipposideros speoris* and *Megaderma lyra*. J Comp Physiol A163:271–285.

Rutkowski RG, Wallace MN, Shackleton TM, Palmer AR. 2000. Organisation of binaural interactions in the primary and dorsocaudal fields of the guinea pig auditory cortex. Hear Res 145:177–189.

Schuller G, O'Neill WE, Radtke-Schuller S. 1991. Facilitation and delay sensitivity of auditory cortex neurons in CF-FM bats, *Rhinolophus rouxi* and *Pteronotus p. parnellii*. Eur J Neurosci 3:1165–1181.

Shen JX, Chen QC, Jen PH. 1997. Binaural and frequency representation in the primary auditory cortex of the big brown bat, *Eptesicus fuscus*. J Comp Physiol A181:591–597.

Shen W. 1996. The medial geniculate body of the pallid bat: cytoarchitecture and connectivity with the auditory cortex. Master's Thesis, University of Wyoming.

Suga N. 1989. Principles of auditory information-processing derived from neuroethology. J Exp Biol 146:277–286.

Tanaka K, Otani K, Tokunaga A, Sugita S. 1985. The reciprocal connec-

tions of the suprageniculate nucleus and the superior colliculus in the rat. Neurosci Res 3:79–85.

Velenovsky DS, Cetas JS, Price RO, Sinex DG, McMullen NT. 2003. Functional subregions in the primary auditory cortex defined by thalamocortical terminal arbors: an electrophysiological and anterograde labeling study. J Neurosci 23:308–316.

Wenstrup JJ. 1999. Frequency organization and responses to complex sounds in the medial geniculate body of the mustached bat. J Neurophysiol 82:2528–2544.

Wenstrup JJ, Grose CD. 1995. Inputs to combination-sensitive neurons in the medial geniculate body of the mustached bat: the missing fundamental. J Neurosci 15:4693–711.

Wenstrup JJ, Larue DT, Winer JA. 1994. Projections of physiologically defined subdivisions of the inferior colliculus in the mustached bat: targets in the medial geniculate body and extrathalamic nuclei. J Comp Neurol 346:207–236.

Wepsic JG. 1966. Multimodal sensory activation of cells in the magnocellular medial geniculate nucleus. Exp Neurol 15:299–318.

Winer JA, Sally SL, Larue DT, Kelly JB. 1999. Origins of medial geniculate projections to physiologically defined zones of rat primary auditory cortex. Hear Res 130:42–61.

Winer JA, Miller LM, Lee CC, Schreiner CE. 2005. Auditory thalamocortical transformation: structure and function. Trends Neurosci 28:255–263.